

MOLECULAR DYNAMICS SIMULATIONS OF DISPLACEMENT CASCADES IN FE-10%CR SYSTEMS

G. Yu¹, D.G. Lu¹, Y. Ma¹, J. Cai¹ and R. Schaeublin²

¹ North China Electric Power University, Beijing, China

² CRPP - EPFL, Villigen PSI, Switzerland

Abstract

Molecular Dynamics (MD) simulations of displacement cascades in Fe-10%Cr systems are used to simulate the Primary Knocked-on Atom (PKA) events on the irradiation damage at temperature 300, 600 and 750K with PKA energies between 1 and 15keV. The results indicate that the vacancies produced by cascade are all in the central region of the displacement cascade. During the cascade evolution all recoil Fe and Cr atoms combine with each other to form Fe-Cr or Fe-Fe interstitial dumbbells as well as interstitial clusters. The number and size of interstitial clusters increase with the energy of PKA and temperature. A few large clusters consisting of a large number of Fe interstitials with a few Cr atoms, the rest being Fe-Cr clusters with small and medium sizes. The interstitial dumbbells of Fe-Fe and Fe-Cr are in the $\langle 111 \rangle$ and $\langle 110 \rangle$ series direction, respectively.

1. Introduction

High-Cr Ferritic/Martensitic (F/M) steels are primary candidate structural materials for future nuclear power plants, due to their good void swelling resistance and superior mechanical properties [1]. In future nuclear systems it is expected that core structural materials will be subjected to severe irradiation and environmental conditions during the reactor life-time [2]. Irradiation, in general, leads to a degradation of the mechanical properties of materials, via creation of radiation defects and secondary phase particles, both of them hindering the motion and creation of dislocations in metals and alloys. A quantitative understanding of the mechanisms leading to the change of properties of these steels after long-term exposure to irradiation is therefore recognized to be of high importance for a safe design and operation of innovative nuclear systems [3].

High-Cr FM steels for nuclear applications, including reduced activation and Oxide-Dispersed Strengthened (ODS), typically contain from 7 to 14 at.% Cr, while the content of the other alloying elements generally does not exceed 1-2%. The main alloying element is Cr and Fe-Cr binary alloys can be used as model materials to study the behaviour of these steels. The degradation of material properties under irradiation is a multi-scale phenomenon, meaning that different physical processes take place on different time and space levels. Nowadays, it is widely accepted that a multi-scale modelling approach provides a practical framework to tackle this problem. This approach begins with the production of atomic-scale defects by individual displacement cascades and ends with plasticity and fracture mechanics treatment of whole components, wherein the response of the material to changes in temperature and/or applied stress is of concern [4]. In this framework, Molecular Dynamics (MD) techniques are a unique tool for studying the primary damage state due to displacement cascades induced by high energy particles (such as neutrons, ions, electrons, etc.). Over the last decade MD simulations have been widely used to assess the primary damage state in pure bcc Fe [5], some Fe-based systems [6-8], and also Fe-Cr alloys [9-13]. Simulations of displacement cascades in Fe-Cr random alloys have been carried out mostly in Fe-10%Cr alloys [9-12], and these simulations could only be reliably performed for a Cr concentration (C_{Cr}) of 10%,

since this was the only concentration that was acceptably described. In the other hand, in alloys with $C_{Cr} < 10\%$ a tendency towards ordering of Cr atoms is experimentally detected [14, 17]. Note that both of these processes take place in the region of temperatures potentially important for technological applications (above 600K). Moreover, phase transformation can be accelerated under irradiation [15, 16] due to self diffusion via radiation-induced defects and, possibly, also to direct in-cascade atomic redistribution.

In this work, we study the primary damage state in Fe-Cr binary alloys with temperature dependence, addressing the following issues:

- (i) Whether does the presence of Cr affect the number of formed Frenkel pairs and their clustering in the region of temperatures potentially important for technological applications (above 600K)?
- (ii) Whether are different the cluster characters in the results of cascade at room temperature and the temperature region in technological applications (above 600K)?
- (iii) Is the in-cascade ballistic mixing sufficient to induce, within the short time frame of the cascade, Cr atom redistribution as dictated by the acting thermodynamic forces (i.e. the heat of mixing of the corresponding alloy)?

In present MD calculation to 20ps, the primary damage process and state of displacement cascades by MD techniques experiences the ballistic collision in 10^{-6} -0.2ps, displacement spike formation (local explosion, shock wave, melting to low density droplet) in 0.2-0.3ps, relaxing (driving out Self Interstitial Atoms (SIAs), atomic mixing and transferring to super-cooling droplet) in 0.3-3ps, solidifying and cooling to circumstance temperature in 3-10ps (forming deleted zone, disorder (or amorphous) region, vacancies-plate collapse etc.) [18, 19] and following diffusion process in 10-20ps. Therefore it is able to address above mentioned issues, especially to address the primary damage state at high temperature to be different than that at low temperature (including the short term diffusion process at circumstance temperature after completing whole process of displacement spike).

2. Cascade generation models and analysis methods

Cascade generation models and analysis methods were used as MD with the MOLDY [20], periodic boundary conditions were imposed on a constant pressure ensemble of atoms with simulation cells containing 0.5 million atoms for the highest energy 15keV simulations. A Fe-Cr simulation cell with 10% Cr in random body-centre cubic (bcc) lattice positions was created. The interatomic potentials used were the PAW version (based on projector augmented wave density functional theory results) of the Fe-Cr potential by Olsson et al. [21] which was developed to be used together with the Olsson Cr-Cr potential [21] and the Ackland-Mendelev 2004 Fe-Fe potential [22]. The coefficients of the alloy potential were fitted to the lattice parameter, 0.28553nm, of Fe90%-Cr10%, a positive heat of mixing for equimolar composition, the binding energy of the mixed <110>-dumbbell in bulk Fe, the substitution energy of a Cr atom in bulk Fe, and the mixing enthalpy curve.

At the beginning of the simulation, the system of particles was equilibrated for 2ps at a temperature representative of operating conditions, such as 300, 600 and 750K (~the well-known 475°C (748K) embrittlement of high-Cr Fe-Cr alloys due to nano-segregation of chromium). When the lattice was at thermal equilibrium, one atom, the PKA was given a momentum corresponding to an energy of 1keV or others. The time step in the simulation was manually adapted to the PKA velocity, and it

could be as low as 10^{-17} s. Once the cascade energy had been mostly dissipated in elastic collisions, a much longer time step was allowed, i.e. 10^{-16} - 10^{-15} s. More details on the procedure can be found in [23].

The cascades were then started by choosing a Fe atom near the center of the cell as the PKA and giving it a recoil energy, such as 1keV or others. The direction of the recoil was random. Temperature scaling (with a constant of 100fs) was applied in the cell's border regions (with a thickness of one lattice parameter). The simulation was stopped if the kinetic energy of a border atom was larger than 10eV and restarted with the recoil atom placed farther away from the border but keeping the recoil direction the same. The simulation time was 20ps. The volume was kept constant, and the temperature was scaled at the borders to remove heat from the system.

To analyze the defects a Wigner-Seitz cell, centred at each lattice site, was used: an empty cell corresponded to a vacancy, while two atoms in the same cell were a self-interstitial configuration. We performed a cluster connectivity analysis, which means that a group of defects are interpreted to belong to the same cluster if they are within a given distance from at least one other defect of the same type. This distance is called a (clustering) cut-off radius. The choice of the cut-off radius is governed by the presence of some significant binding energy between alike defects, which is the 2nd nearest neighbour (nn) for vacancy defects, and the 3rd nn for SIA defects. Special attention was paid to the fraction of clustered SIAs and vacancies, as well as to the Cr content among SIAs and clustered SIAs.

In order to make the statistical average for the number of surviving Frenkel pairs and defect clusters produced by the cascade with MD simulation, the number of cascades, simulation time and box size for various temperature and PKA energy E_{MD} are summarized in Table1.

E_{MD} (keV)	No. of cascades in Fe-10%Cr			Other parameters	
	300K	600K	750K	Time (ps)	Box size (atoms)
1	10	10	10	20	500,094
5	10	10	10	20	500,094
10	10	10	10	20	500,094
15	10	10	10	20	500,094

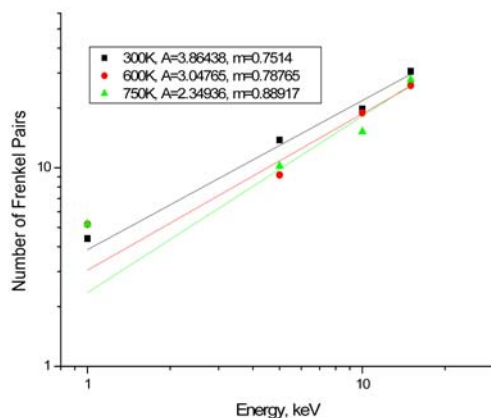
Table1 Summary of number of cascades, simulation time and box size versus temperature and E_{MD}

3. Results and discussion

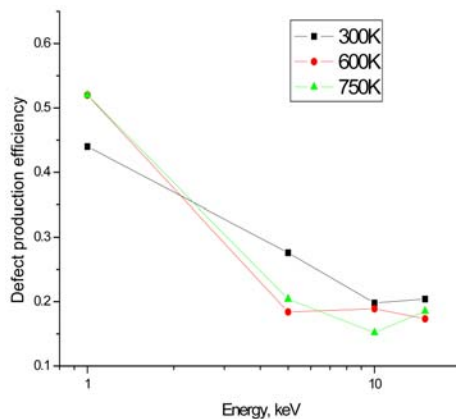
3.1 Defect number

The average Number of surviving Frenkel Pairs (N_{FP}) for various temperatures at the end of cascade in Fe-10%Cr resulting from the MD simulations is plotted as a function of E_{MD} , shown in Figure 1(a). The points have been interpolated using the empirical power law proposed by Bacon et al., $N_{FP} = A \cdot E_{MD}^m$ [24]. Prefactors A and exponents m obtained in a least-square fit are agreement with previous work on Fe [25]. The exponent increases with the temperature from 0.7514 at 300 K to 0.8892 at 750 K. This means that the defect production is more sensitive to PKA energy at 750 K in Fe-10%Cr. Traditionally, the number of Frenkel pairs produced per cascade is estimated using [26]

the NRT formula, $N_{NRT} = 0.8E_D/2E_d$, where E_d is the average displacement energy for all crystallographic directions and E_D is the PKA energy. E_D is the fraction of recoil energy that goes into displacement damage, after subtracting the fraction dissipated for electron excitation. Since in the present MD simulations the interaction between ions and electrons is not included, it is assumed that $E_D = E_{MD}$. The defect production efficiency is defined as the ratio of the surviving MD Frenkel pairs to the number of NRT displacements (N_{FP}/N_{NRT}). For the sake of comparison, we took $E_d = 40$ eV to estimate the number of defects with the NRT formula. The defect production efficiency shown in Fig. 1(b), decreases with recoil energy to a more or less asymptotic value of about 0.22 on 10keV at 300K and 0.20 on 5keV at 750K. The asymptotic value of defect production efficiency is not sensitive to temperature above 300K, but the start point (PKA energy) of asymptotic curve decreases with the operation temperature increase. These results are similar to the results in the pure iron [25] and the asymptotic value of defect production efficiency is reasonable, which is similar and close to the experimental value about the fraction of the number of survive defects in irradiated metals on the normal temperature (about 0.15) [18].



(a)



(b)

Figure 1 Number of surviving Frenkel pairs (a) and defect production efficiency compared to NRT (b) at the end of the cascade versus recoil energy, in Fe-10%Cr with various temperatures.

In (a) the power law proposed by Bacon et al., $N_{FP} = A \cdot E_{MD}^m$, has been used for interpolation.

The present potential predicts a positive binding energy of the mixed $\langle 110 \rangle$ -dumbbell in bulk Fe. This feature leads to the formation of a number of mixed dumbbells, the fraction of Fe-Cr interstitials in the total number of interstitials is remarkably higher than the fraction of Cr in matrix at the end of the cascade, as is shown in Figure 2. Above 5keV of the recoil energy, more than 20% of the final dumbbells contain Cr atoms, to be compared with the 10%Cr concentration of the alloy. Below 5keV of the recoil energy the formation of mixed dumbbells increases with the operation temperature. Initially, as is to be expected, more Fe atoms than Cr atoms are displaced and counted as interstitials. However, during the cooling stage most of these Fe-Fe dumbbells, possibly assisted by the still high temperature, glide till they become trapped at the closest Cr atoms, thereby determining the number of mixed and self-interstitial dumbbells at higher temperature more than that of normal temperature. But the recoil energy higher than 5keV, the displacement spike is large enough and the in-cascade ballistic mixing sufficient to induce, within the short time frame of the cascade, Cr atom redistribution as dictated by the acting thermodynamic forces (i.e. the heat of mixing of the corresponding alloy) to be advantage to Fe-Cr interstitials formation. In summary: Cr atoms do not appear to significantly affect the collisional stage of the cascade, as may be expected, considering the negligible difference in mass between Fe and Cr atoms. Yet, the presence of Cr determines a redistribution of dumbbell species during the post-collisional stage, where the dumbbells is advantage to contain Cr atoms, in percentage far higher than the Cr concentration in the alloy, i.e. the fraction of Fe-Cr dumbbells in the total interstitials dumbbells is higher than 10%, produced by the cascade. The direction of Fe-Cr dumbbell is along $\langle 110 \rangle$, same as the direction of Fe-Fe dumbbell along $\langle 110 \rangle$, which is in agreement with *ab initio* calculation [15].The thermal stability of these dumbbells is likely to be responsible for Figure 2. The fraction of Fe-Cr and Cr-Cr dumbbells in Fe-10%Cr cascades versus recoil energy with various operation temperatures (average evolution of 10 cascades). It indicates that the $\langle 110 \rangle$ Fe-Cr and Cr-Cr dumbbells are more stable than the corresponding defect in pure iron. Consequently, Cr would tend to end up in defect structures forming during the cooling down of recoil cascades.

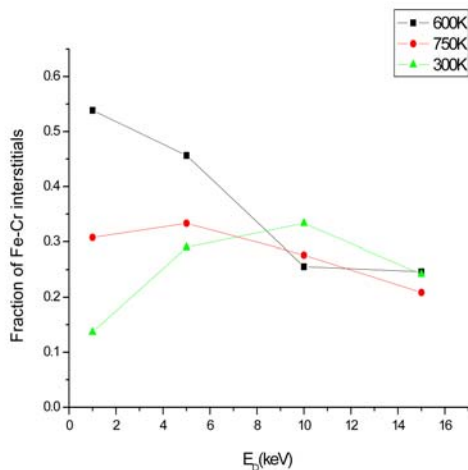


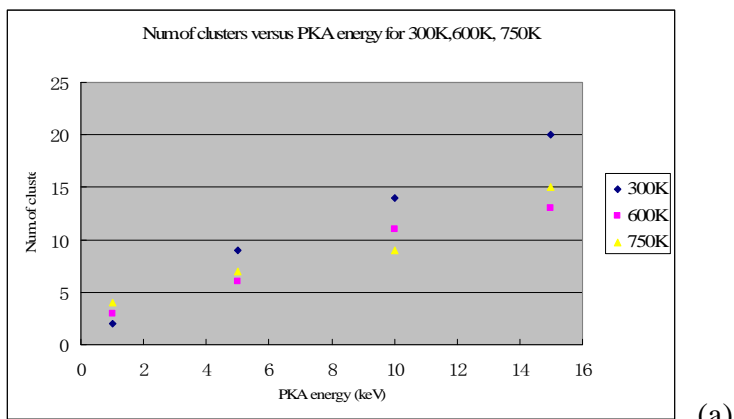
Figure 2 The fraction of the number of Fe-Cr dumbbells interstitials to the number of interstitials versus PKA's energy for various temperatures.

3.2 Cluster formation

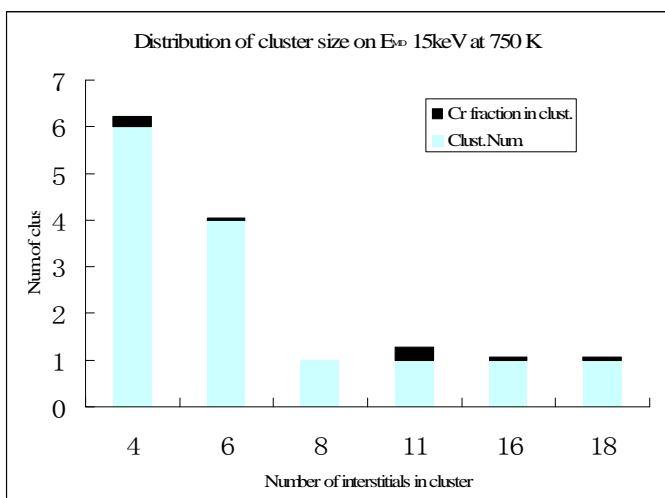
Previous papers on displacement cascades in Fe show that very little in-cascade vacancy clustering occurs in this material, while sizeable interstitial clusters are found [11, 23-25, 27]. Our results agree with these findings. The number of interstitial clusters versus PKA energy E_D for various temperature and the size distribution of clusters for E_D as 15keV at 750K are shown in Figure 3(a) and (b), which sums the number and size of interstitial clusters of 5 events for one case, which is corresponding to 5 cascades with random emitted direction in one region with time interval 10ps. The results presented are for a distance between neighbours of 0.49455 nm (3rd nn). In this calculation, we consider a cluster those that contain more than 3 interstitials. The calculation results indicate that the number and size of interstitial clusters increases with the energy of PKA and is not sensitive to temperature in the range 300-750K at the PKA energy above 5keV. The most of clusters in size is less than 8 interstitials, but there are always a few larger clusters with some Cr interstitials. The clusters seem to be stabilized by the Fe-Cr mixed interstitial. The Cr fraction distribution in small clusters is shown in Figure 3(c), it shows that the peak of Cr fraction is at 0.25 to be higher than that in matrix.

Interstitial clusters can be formed in cascades according to at least three mechanisms. They may be formed when a high-density part, produced during the ballistic phase and lingered on into the nearly melted zone created by the displacement spike, is isolated by a re-crystallisation front [28]. Partly they may also form at the end of the displacement spike, as a consequence of collective atomic motion in conditions of enhanced defect diffusion, due to high local temperature [29]. Finally, further interstitial clusters formation and growth may occur by later local defect re-organization, driven by strain-field interaction among neighbouring interstitials and small clusters [29]. While the presence of interstitial-trapping solute atoms can hardly affect the first of these mechanisms, the other two are expected to be greatly influenced by it. But the Fe $\langle 111 \rangle$ crowdions and recoils meeting the Cr atom will be 'broken' to form the mixed dumbbell, the mixed dumbbell migration will not only enhance the effective stability of mixed dumbbells, but also favour the formation of clusters containing a significant amount of Cr atoms by aggregation of single interstitials under the high local temperature of displacement spike region. Thus there are many small clusters to be stable at end of cascade step, which contains Cr as shown in Figure 3(c).

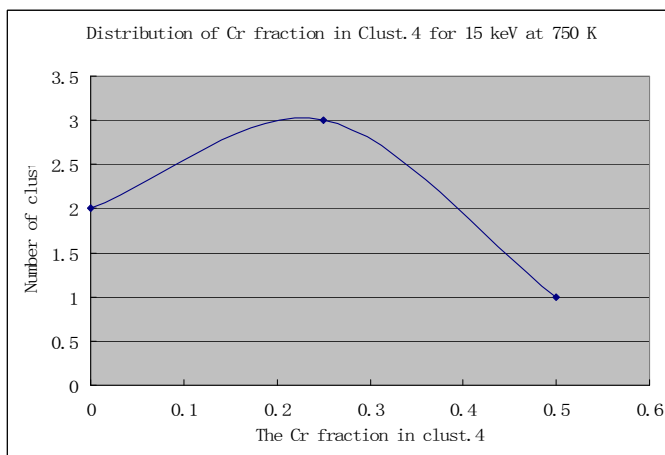
At the same time, the large clusters formed in cascades will still be of $\langle 111 \rangle$ type Fe crowdions which can efficiently gather and form clusters, and will still fast glide one-dimensionally toward regions of high Cr concentration, where they will get trapped. Thus, more interstitials in clusters means globally less 'free' single interstitials suitable for being 'captured' by Cr atoms and, therefore, less Cr atoms in interstitial position. Interstitial clusters are formed in cascades in Fe partly at an early stage as a consequence of re-crystallization, partly at the end of the displacement spike, as a consequence of collective atomic motion, and partly later, via local defect re-organization, driven by elastic interactions among interstitial defects.



(a)



(b)



(c)

Figure 3 The number of interstitial clusters versus PKA energy for 300 , 600 and 750 K (a); their size distribution of cluster in E_D 15keV at 750K (b); the number of interstitial clusters distribution versus the fraction of $N_{Cr}/N_{interstitial}$ in clusters (containing the 4 interstitials) on 15keV at temperature 600K (c)

We expect that the formation of Fe-Cr mixed interstitial clusters, which are shown here to be stabilized by Cr, will have a large impact on the subsequent evolution of radiation damage. Because single interstitials in Fe-Cr migrate three-dimensionally, maintaining a $\langle 110 \rangle$ dumbbell configuration, with a migration energy of about 0.3eV, these slowly migrating single $\langle 110 \rangle$ dumbbells lead to diffuse into Fe-Cr mixed interstitial clusters getting growth and their getting trapped at Cr atoms to evolve more larger Fe-Cr mixed interstitial clusters. Because three-dimensionally migrating interstitials have any way, in the long term, more chances of finding a trap than one-dimensionally migrating ones and, in addition, differently from solute-centred crowdions, mixed dumbbells can migrate as such, i.e. once the mixed dumbbell is formed it will not be 'broken' by the process of interstitial migration. This possibility of mixed dumbbell migration will not only enhance the effective stability of mixed dumbbells, but also favour the formation of clusters containing a significant amount of Cr atoms by aggregation of single interstitials.

These Fe-Cr mixed interstitial clusters may be obstacles to dislocation motion, leading to hardening associated with a DBTT shift. The observed large amount of small sized Fe-Cr mixed interstitial clusters may help explain the experimental observations. A high density of defects with mean size range in 1.5-6.9 nm was observed, but no cavities, even at the highest studied dose [30]. At operation temperature ($>350^\circ\text{C}$) the Fe-Cr mixed interstitial clusters will evolve to nanometric dislocation loops with a Burgers' vector $\mathbf{b} = \frac{1}{2}a_0\langle 111 \rangle$ in the $\{111\}$ plane. At well-known 475°C (748K) embrittlement of high-Cr Fe-Cr alloys is due to nano-segregation of chromium. We predict that the $\langle 110 \rangle$ Fe-Cr and Cr-Cr dumbbells are more stable than the corresponding defect in pure iron. Consequently, Cr would tend to end up in defect structures forming during the cooling down of recoil cascades.

3.3 The configuration of clusters

The configuration of 10keV cascade at 600K on 10 and 20ps are shown in Figure 4(a) and (b). There are no significant difference between Figure 4(a) and (b). As we predict, before 10ps the cascade experiences the ballistic collision (10^{-6} -0.2ps), displacement spike process (0.2-3ps) and solidifying and cooling to circumstance temperature in 3-10ps. The surviving defects are stable, as shown in Figure 4(a), then follow the diffusion process in 10-20 ps. The period in 10-20ps is too short, the surviving defects migrate to be not too far and the agglomeration to be limited, except the high speed migration of special defects, such as $\langle 111 \rangle$ crowdions. Therefore the configuration of cascade at 20ps is able to be described as the primary damage characterization and features of cascade, such as vacancies spatial distribution, vacancy clusters size and spatial distribution, dumbbell interstitials spatial distribution, interstitial clusters size and spatial distribution, the composition in interstitial cluster and interstitial cluster shape (such as nanometer interstitial loops), etc. as a record database for analysis and entering next code, such as Object Kinetic Monte Carlo (OKMC) method [31] for microstructure evolution calculation.

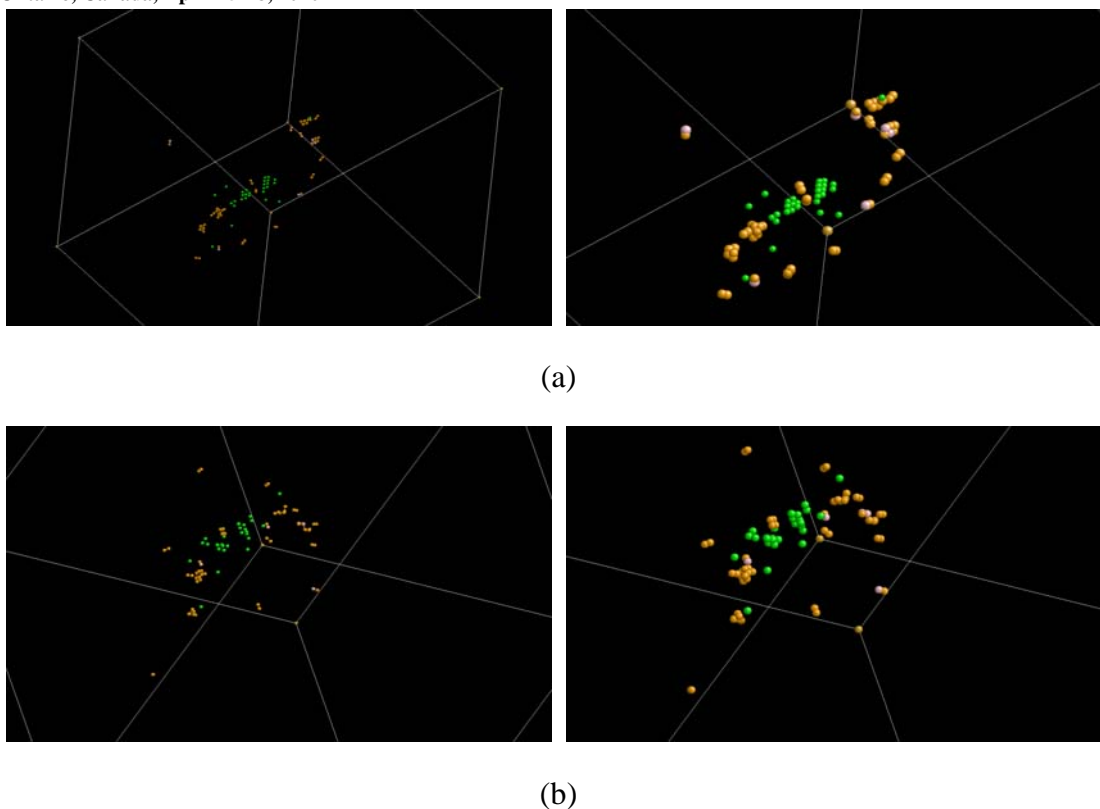


Figure 4 The configuration of 10 keV cascade on 10ps (a) and 20ps (b) at 600K, including vacancies spatial distribution, vacancy clusters size and spatial distribution, dumbbell interstitials spatial distribution, interstitial clusters size and spatial distribution, the composition in interstitial cluster and interstitial cluster shape (such as nanometer interstitial loops), and its spatial clusters.

4. Summary

- 1) Using Ackland-Mendelev 2004 Fe-Fe potential, Olsson Fe-Cr and Cr-Cr potential and MD with the MOLDY code calculated the average number of surviving Frenkel pairs (NFP) and defect production efficiency versus PKA energy at 300, 600 and 750K. The defect production efficiency decreases with recoil energy to a more or less asymptotic value of about 0.22 on 10keV at 300K and 0.20 on 5keV at 750K. The asymptotic value of defect production efficiency is not sensitive to temperature above 300K, but the start point (PKA energy) of asymptotic curve decreases with the operation temperature increase. The asymptotic value of defect production efficiency is similar and close to the experimental values about the fraction of the number of survive defects in irradiated metals on the normal temperature.
- 2) At the end of the cascade, the interstitials are all belong to $\langle 110 \rangle$ -dumbbell and the fraction of Fe-Cr mixed interstitials in the total number of interstitials is remarkably higher than the fraction of Cr in matrix. Above 5keV of the recoil energy, the displacement spike is large enough, Cr atom redistribution as dictated by the acting thermodynamic forces to be advantage to Fe-Cr interstitials formation, more than 20% of the final dumbbells contain Cr atoms, to be compared with the 10% Cr concentration of the alloy. It indicates that the $\langle 110 \rangle$ Fe-Cr and Cr-Cr dumbbells are more stable than the corresponding defect in pure iron.

- 3) The number and size of interstitial clusters increases with the energy of PKA and is not sensitive to the temperature in the range 300-750 K. A few large interstitial clusters is Fe cluster formed by high speed $\langle 111 \rangle$ crowdions accumulation. The most of interstitial clusters is Fe-Cr mixed interstitial clusters, which may be obstacles to dislocation motion, leading to hardening associated with a DBTT shift. The observed large amount of small sized Fe-Cr mixed interstitial clusters may help explain the experimental observations. A high density of defects with mean size range in 1.5-6.9 nm was observed, but no cavities, even at the highest studied dose.
- 4) The configuration of 10keV cascade at 10 and 20ps indicates that there is no significant difference between them. During 10ps period the cascade completed the ballistic collision, displacement spike process and solidifying and cooling to circumstance temperature, the surviving defects are stable. After another 10ps, the surviving defects further evolving to the stable configuration, which is able to be described as the primary damage characterization and features of cascade.

5. References

- [1] R. Klueh, D. Harries, High-Chromium Ferritic and Martensitic Steels for Nuclear Applications, ASTM Intl., 2001, p. 337.
- [2] L.K. Mansur, A.F. Rowcliffe, R.K. Nanstad, S.J. Zinkle, W.R. Corwin, R.E. Stoller, J. Nucl. Mater. 329–333 (2004) 166.
- [3] S.J. Zinkle, Phys. Plasmas 12 (2005) 058101.
- [4] B.D. Wirth, M.J. Caturla, T. Diaz de la Rubia, T. Khraishi, H. Zbib, Nucl. Instrum. and Meth. B 180 (2001) 23.
- [5] L. Malerba, J. Nucl. Mater. 351 (2006) 28.
- [6] A.F. Calder, D.J. Bacon, Mater. Res. Soc. Symp. 439 (1997) 521.
- [7] A.F. Calder, D.J. Bacon, A.V. Barashev, Y.N. Osetsky, Philos. Mag. Lett. 88 (2008) 43.
- [8] C.S. Becquart, C. Domain, J.C. Van Duysen, J.M. Raulot, J. Nucl. Mater. 294 (2001) 274.
- [9] D. Terentyev, L. Malerba, R. Chakarova, C. Domain, K. Nordlund, P. Olsson, M. Rieth, J. Wallenius, J. Nucl. Mater. 349 (2006) 119.
- [10] C. Björkas, K. Nordlund, L. Malerba, D. Terentyev, P. Olsson, J. Nucl. Mater. 372 (2008) 312.
- [11] L. Malerba, D. Terentyev, P. Olsson, R. Chakarova, J. Wallenius, J. Nucl. Mater. 329–333 (2004) 1156.
- [12] J.-H. Shim, H.-J. Lee, B.D. Wirth, J. Nucl. Mater. 351 (2006) 56.
- [13] J. Wallenius, P. Olsson, C. Lagerstedt, N. Sandberg, R. Chakarova, V. Pontikis, Phys. Rev. B 69 (2003) 094103.
- [14] I. Mirebeau, M. Hennion, G. Parette, Phys. Rev. Lett. 53 (1984) 687.
- [15] P. Dubuisson, D. Gilbon, J.L. Séran, J. Nucl. Mater. 205 (1993) 178.
- [16] M.H. Mathon, Y. de Carlan, G. Geoffroy, X. Averty, A. Alamo, C.H. de Novion, J. Nucl. Mater. 312 (2003) 236.
- [17] N.P. Filippova, V.A. Shabashov, A.L. Nikolaev, Phys. Met. Metall. 90 (2000) 145.
- [18] Jinnan Yu, Radiation Effects on Materials, Chemical Industry Publishing House, Beijing, 2007
- [19] C. Björkas, K. Nordlund, L. Malerba, D. Terentyev, P. Olsson J. Nucl. Mater. 372 (2008) 312–317
- [20] M.W. Finnis, 'MOLDY6-A Molecular Dynamics Program for Simulation of Pure Metals,' AERE R-13182, UKAEA Harwell Laboratory, Harwell, UK, 1988.
- [21] P. Olsson, J. Wallenius, C. Domain, K. Nordlund, L. Malerba, Phys. Rev. B 72(2005) 214119.

- [22] G.J. Ackland, M.I. Mendeleev, D.J. Srolovitz, S. Han, A.V. Barashev, J. Phys.:Condens. Matter 16 (27) (2004) S2629
- [23] C.S. Becquart, C. Domain, A. Legris, J.C. Van Duysen, J.Nucl. Mater. 280 (2000) 73
- [24] D.J. Bacon, A.F. Calder, F. Gao, et al., Nucl. Instrum. And Meth. B 102 (1995) 37
- [25] R.E. Stoller, J. Nucl. Mater. 276 (2000) 22
- [26] M. Norgett, M. Robinson, I. Torrens, Nucl. Eng. Des. 33 (1975) 50.
- [27] C. Domain et al., J. Nucl. Mater. 335 (2004) 121.
- [28] K. Nordlund, M. Ghaly, R.S. Averback, M.-J. Caturla, T.Diaz de la Rubia, J. Tarus, Phys. Rev. B 57 (1998) 7556.
- [29] D.J. Bacon, A.F. Calder, F. Gao, J. Nucl. Mater. 251 (1997)1
- [30] R. Schaublin, M. Victoria, J. Nucl. Mater. 283–287 (2003)339.
- [31] C. Domain, C.S. Becquart, L. Malerba, J. Nucl. Mater. 335 (2004) 121